Atmospheric
Chemistry
and Physics

Supplement of

Development of aerosol activation in the double-moment Unified Model and evaluation with CLARIFY measurements

Hamish Gordon et al.

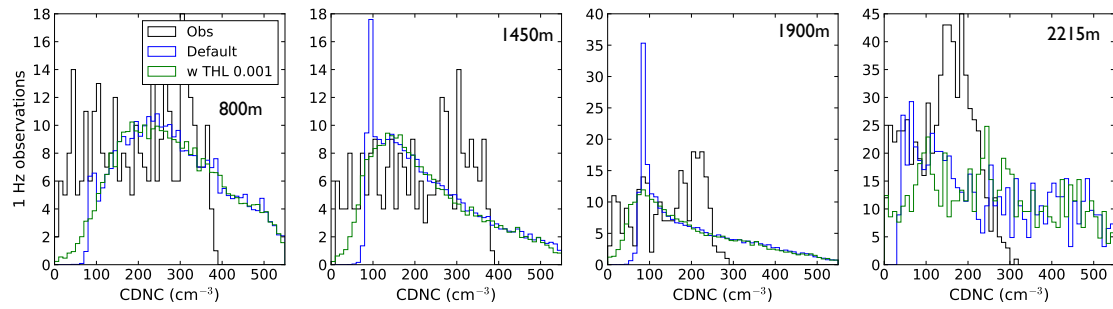*Correspondence to:* Hamish Gordon (hamish.gordon@cern.ch)

Figure S1. Change in droplet concentration (CDNC) when the 'Default' updraft PDF threshold 'THL' of 0.1m/s is reduced to 0.001m/s at 500 m resolution.
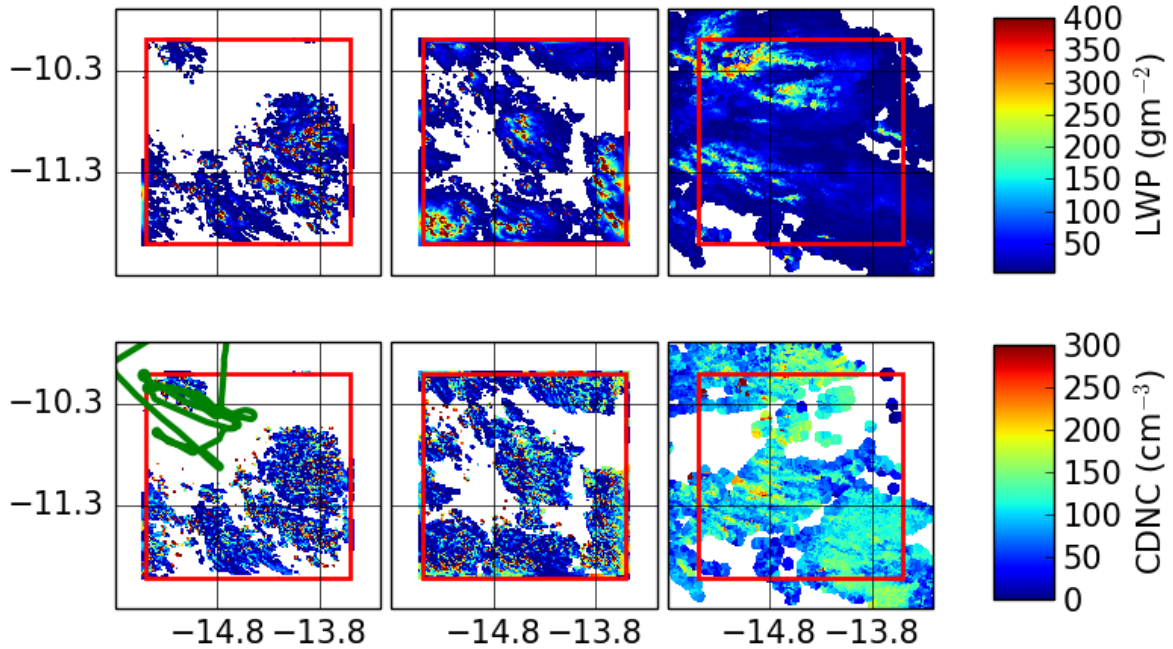
Figure S2. As Figure 3, except that the central subfigures show a new 500 m simulation with the critical relative humidity in the sub-grid cloud scheme lowered by 0.1 (10%) to achieve more cloud cover.

Table S1. Mean in-cloud liquid water content in observations 'Obs' from the cloud droplet probe, compared to the 'Default' version of the model. In both model and observations, the threshold liquid water content is 0.01 g/kg to define a cloud.

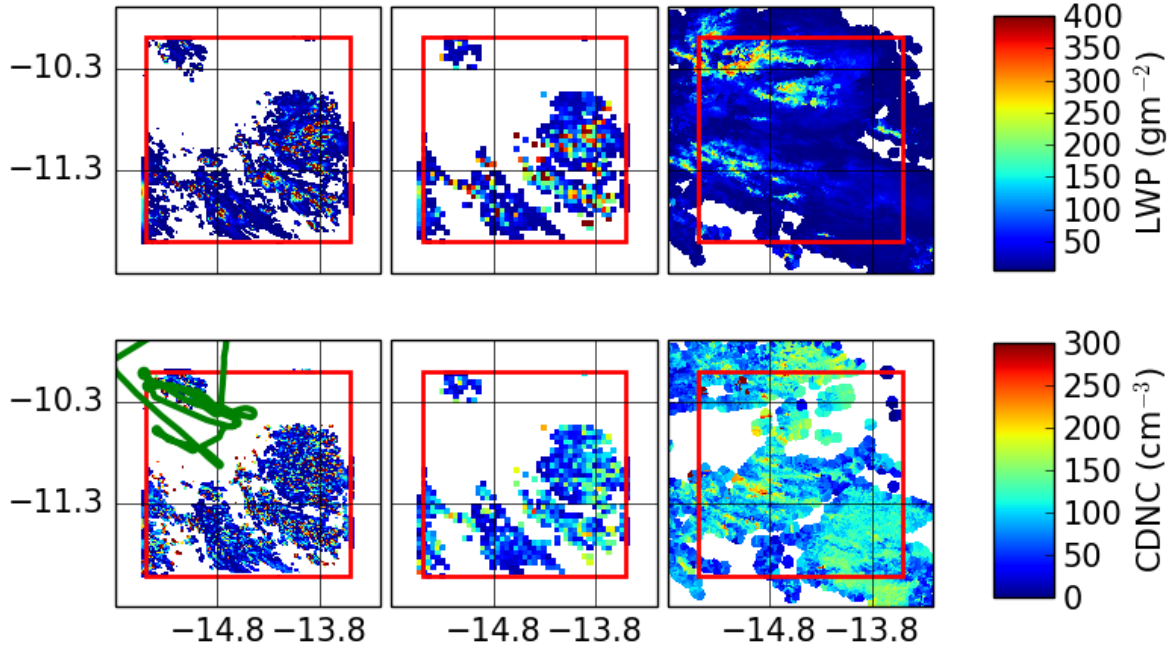| Altitude	Obs (g/kg)	Default (g/kg)
800	0.34	0.07
1450	0.42	0.13
1900	0.58	0.18
2215	0.68	0.58
2550	0.70	0.98

Figure S3. As Figure 3, except that the central subfigures show the 500 m simulation regridded to 5 km resolution, for a potentially fairer comparison with MODIS

Table S2. Mean $\bar{w}$ and standard deviation σ_w of in-cloud vertical velocity w in observations and in simulations, split by liquid water content (LWC) with LWC $> 0.15\,\mathrm{gkg}^{-1}$ above the horizontal line and lower LWC below.

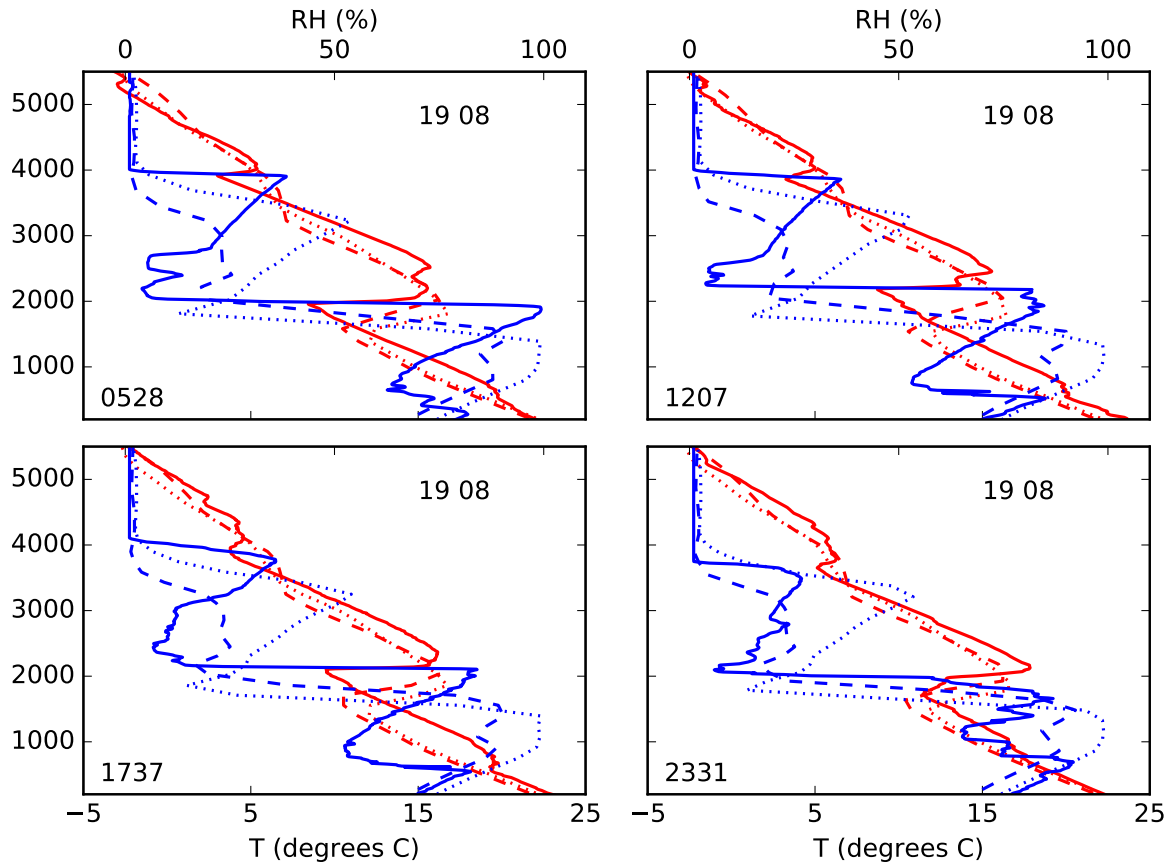| Altitude (m)	$\bar{w}$ obs. ms^{-1}	$\bar{w}$ model ms^{-1}	σ_w obs. ms^{-1}	σ_w 500 m ms^{-1}
800	0.69	0.98	1.32	0.90
1450	0.75	0.51	1.40	0.92
1900	0.72	0.17	1.47	0.73
2215	0.04	0.07	1.63	1.00
2550	-0.61	0.17	2.80	1.37
800	-0.006	0.12	0.88	0.34
1450	-0.12	-0.012	1.10	0.25
1900	-0.88	-0.04	0.92	0.22
2215	-0.42	-0.15	1.39	0.49
2550	-0.90	0.52	2.35	-

Figure S4. Driving model evaluation against temperature T and relative humidity RH from Ascension Island radiosondes on 19 August. The times in UTC of the sonde launches on 19 August 2017 are marked on the bottom-left of each sub-figure. The global model is shown with the dashed line and the 7 km regional model with the dotted line. To reduce computational expense, the domain we simulate at 500 m resolution does not include Ascension Island.

Table S3. Change to simulated number mean droplet radius $\bar{r}$ when the exponential size distribution 'exp' is replaced offline by the size distribution of Morrison and Gettelman (2008), labelled MG08, based on the same moments, and when it is replaced by a gamma distribution with $\mu = 5$, labelled '$\mu = 5$'.

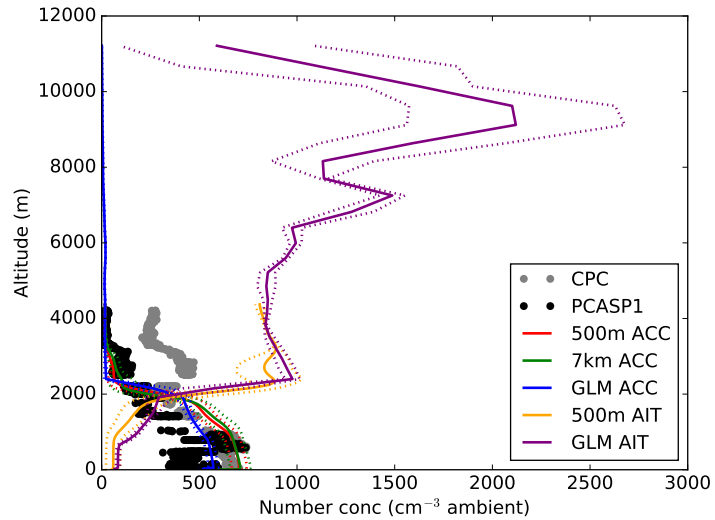| Altitude	$\bar{r}$ (exp) (μm)	$\bar{r}$ (MG08) (μm)	$\bar{r}$ ($\mu = 5$) (μm)
800	2.10	3.44	3.29
1450	2.40	3.89	3.76
1900	2.68	4.39	4.21
2215	3.54	5.60	5.56
2550	4.20	6.06	6.59

Figure S5. Simulated Aitken (AIT) and accumulation-mode (ACC) aerosol number concentrations at ambient temperature and pressure, as in Figure 4, except including the global model (GLM) and extended to high altitudes. The comparison to the CLARIFY PCASP and CPC observations at low altitudes is retained.

.

Table S4. Values of the velocity scaling factor $\sqrt{f/R}$ for a horizontal resolution of $500\,\text{m}$, a factor $f = 4$ correction to the vertical velocity variance suggested by Malavelle et al. (2014), and two boundary layer heights representative of the CLARIFY case study.

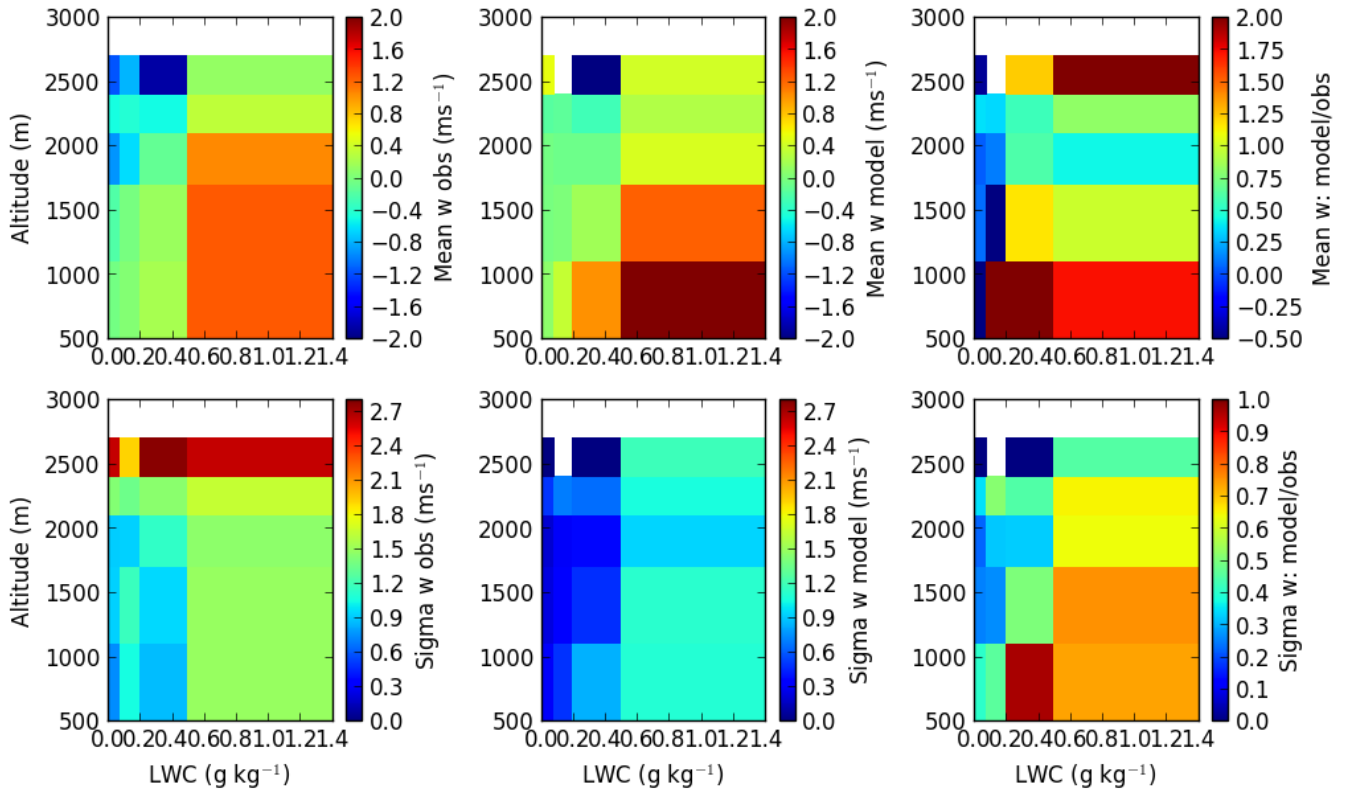| Boundary layer type	Z_{ml}	$\sqrt{f/R}$ ($Z = 1800$m)	$\sqrt{f/R}$ ($Z = 2200$m)
II	$0.5Z$	4.27	3.85
III	$1.3Z$	2.81	2.64
IV	$0.5Z$	4.27	3.85
V (sc)	$0.5Z$	4.27	3.85
V (cbl)	Z	3.09	2.87
VI	Z	3.09	2.87
VII	$0.5Z$	4.27	3.85

Figure S6. Mean and standard deviation of in-cloud vertical velocity w in observations and in simulations, at the usual flight altitudes and in bins of liquid water content (LWC) with boundaries at 0.08, 0.2, and $0.5\,\mathrm{g\,kg^{-1}}$
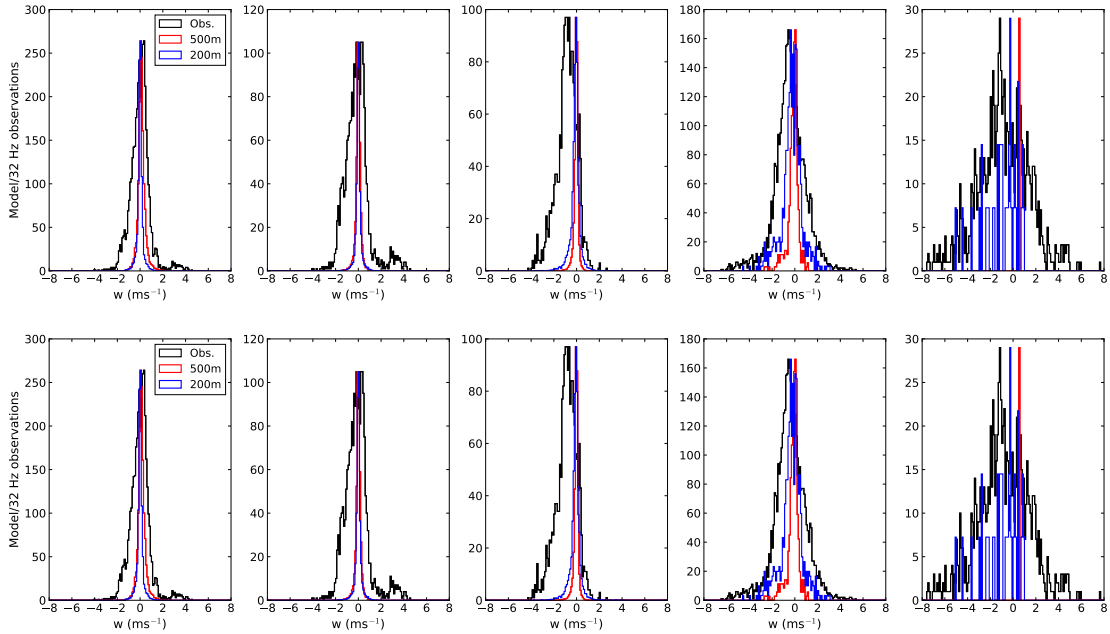
Figure S7. Spatial variability in vertical velocities w in model and observations as PDFs, top for in-cloud LWC$> 0.15\,\mathrm{gkg}^{-1}$ and bottom for LWC$< 0.15\,\mathrm{gkg}^{-1}$. Simulations at $500\,\mathrm{m}$ and $200\,\mathrm{m}$ horizontal resolution are shown, at altitudes of $800\,\mathrm{m}$, $1450\,\mathrm{m}$, $1900\,\mathrm{m}$, $2215\,\mathrm{m}$ and $2550\,\mathrm{m}$ from left to right.
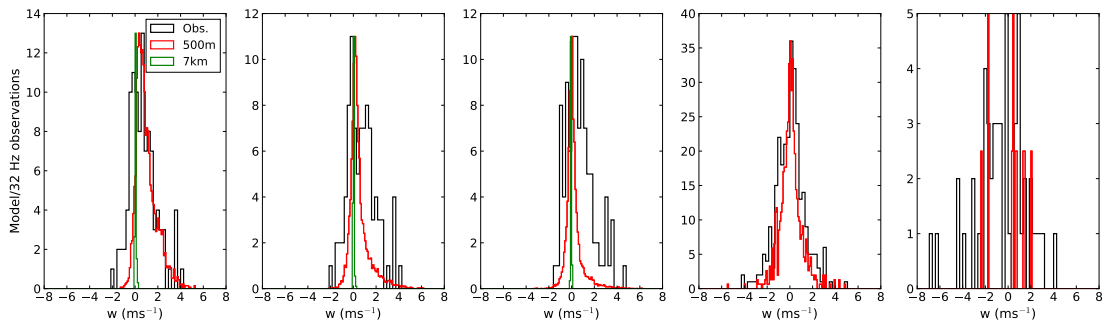

Figure S8. Spatial variability in simulated and observed vertical velocities w that have been smoothed out to average over intervals of $500\,\mathrm{m}$, as PDFs for comparison with the model at this horizontal resolution. Only data for which for in-cloud liquid water content exceeds $0.15\,\mathrm{gkg}^{-1}$ are shown.
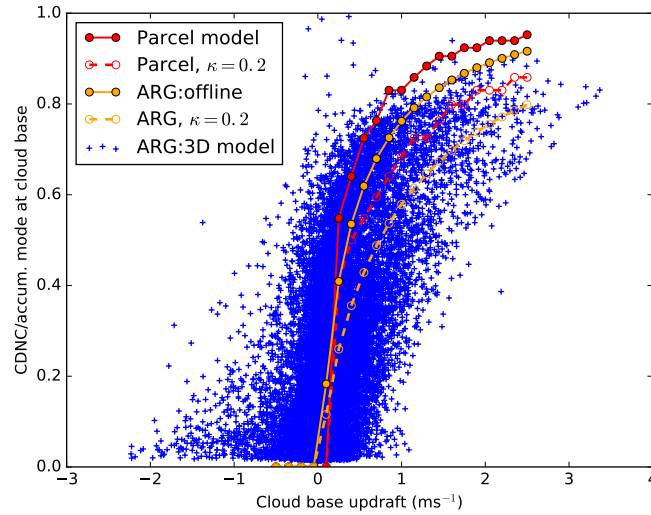
Figure S9. Activated fraction of accumulation-mode aerosols as a function of updraft speed in our 200 m-resolution simulation, in the cloud parcel model of Rothenberg and Wang (2016), and in the ARG parameterization run offline. The aerosol in the parcel model is assumed to be ammonium sulfate, but the dashed lines show additional calculations where the hygroscopicity, represented by the kappa value, is adjusted to 0.2 to represent organic aerosols.
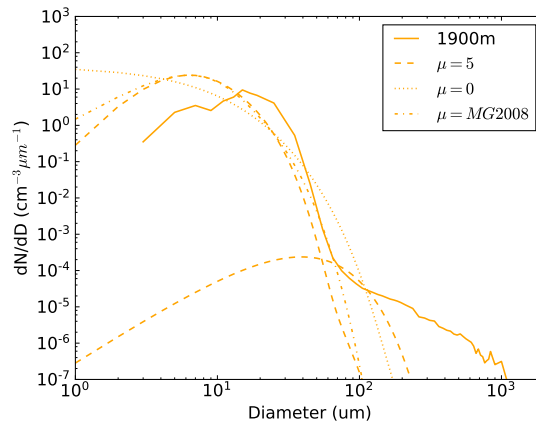

Figure S10. Particle size distributions at 1900 m altitude: observations as in Figure 9, the gamma size distribution with $\mu = 5$ used in this paper (dashed line), the exponential size distribution that was previously in the CASIM code (dotted, labelled $\mu = 0$), and the Morrison and Gettelman (2008) size distribution (dash-dot) that would be derived from the same moments.
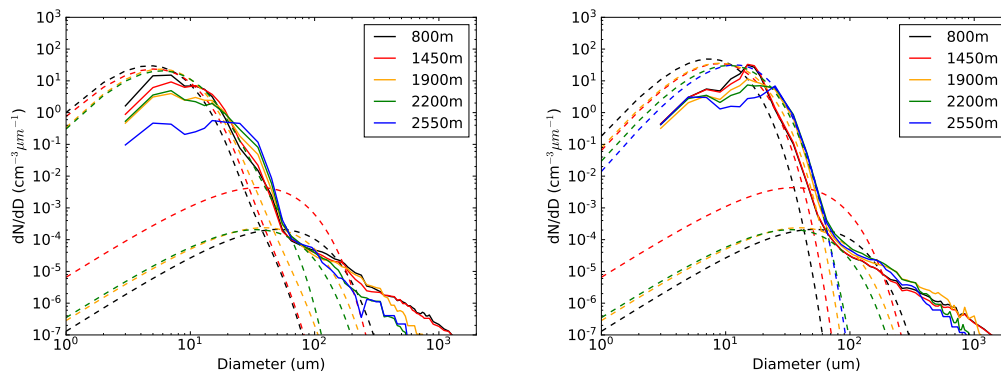
Figure S11. Particle size distributions as Figure 9 except with LWC $< 0.15\,\mathrm{gkg}^{-1}$ (left) and LWC $> 0.15\,\mathrm{gkg}^{-1}$ (right).
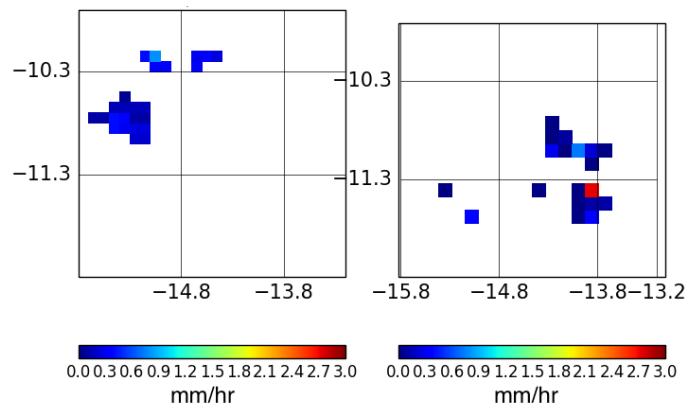

Figure S12. GPM observations of rain (left) compared to simulated rain (right) in the default version of the model.
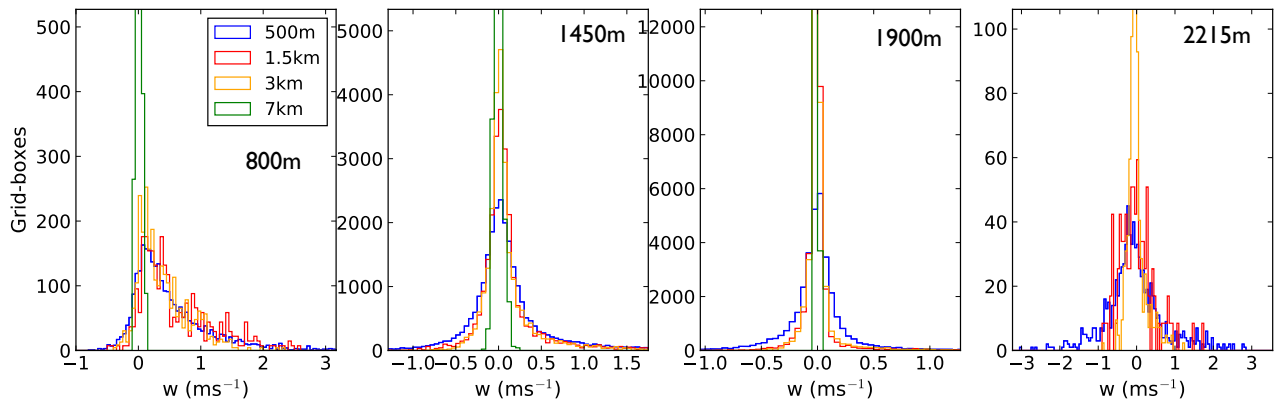
Figure S13. Spatial variability in vertical velocities w as PDFs in simulations at $500\,\mathrm{m}$, $1.5\,\mathrm{km}$ and $3\,\mathrm{km}$ resolution at the altitudes of the four lower straight and level flight legs, where the sample of in-cloud grid boxes is large enough. No threshold liquid water content is applied, and the x axis range is reduced compared to Figure 6 for clarity.
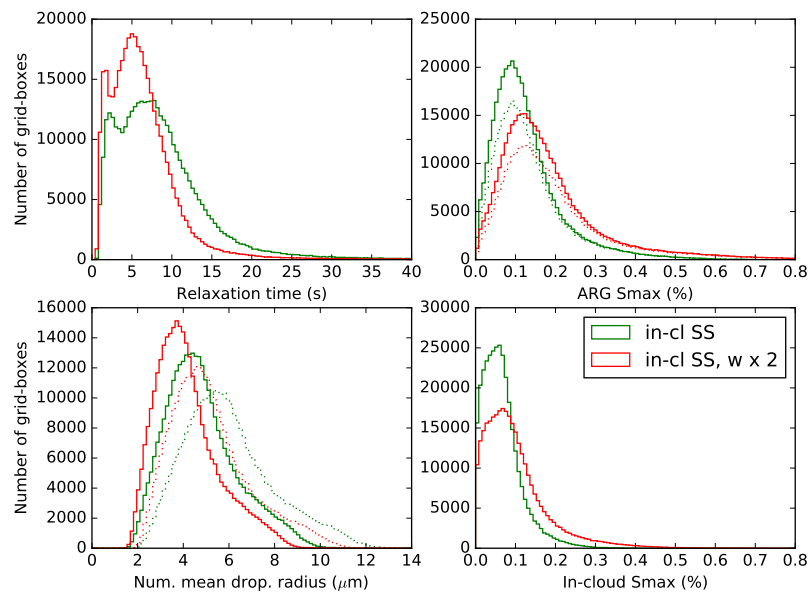

Figure S14. Histograms of grid-box mean relaxation time where relaxation time is used (in grid-boxes where in-cloud quasi-steady super-saturation is used to activate new droplets), ARG maximum supersaturation 'ARG Smax' (on all grid boxes where activation is taking place, and, with dotted lines, on grid boxes where relaxation time is calculated), number mean droplet radius where relaxation time is used, and in-cloud quasi-steady supersaturation 'In-cloud Smax' where it is used. Dotted lines on the plot of number mean droplet radius show effective radius, which is 25% higher.

10

The strange ARG (DIAG) distribution of cloud droplet concentrations

At cloud base, the diagnostic ARG (DIAG) cloud droplet number concentration calculation samples a Gaussian PDF with mean equal to the gridbox mean updraft and width equal to the larger of 0.01 and $\sqrt{2/3TKE}$ (Boutle et al., 2018; Mulcahy et al., 2018), where TKE is the unresolved turbulent kinetic energy. A histogram showing the correlation of the droplet number concentration and the vertical velocity for the lowest 900 m in the model (roughly corresponding to cloud base altitudes), is shown in Supplementary Figure S15. The droplet concentrations and updraft speeds are calculated for 20 bins of the PDF and then the weighted mean is taken:

$$N_d = \frac{\sum N_i p(w_i)}{\sum p(w_i)} \tag{S1}$$

Here $p(w_i)$ is the probability a sub-grid updraft takes the value w_i. So far so good, but this procedure is coded such that the minimum updraft ever sampled from the PDF is zero and the maximum number ever sampled is four times the width, *independently of the mean of the PDF*. The maximum value of $\sqrt{2/3TKE}$ is around 1.2 at cloud base but the mean is around $0.15\,\mathrm{ms^{-1}}$, and so, for example, if the mean updraft speed is less than $-0.45\,\mathrm{ms^{-1}}$ or greater than $1.05\,\mathrm{ms^{-1}}$ (both frequent occurrences in the 500 m resolution simulations) and the width is 0.15, the integral of the PDF between 0 and 0.6 will be essentially zero, as this range is always over 3σ from the mean. The cloud droplet concentration that results will be poorly defined, most likely zero, because one is dividing by zero in the denominator (and multiplying by zero in the numerator) of the weighted mean. The droplet concentration is then reset to its hard-coded minimum of $5\,\mathrm{cm^{-3}}$. The characteristic updraft speed, which is the updraft speed sampled from the PDF that would give the same cloud droplet concentration as the actual weighted mean concentration, will be zero if the real updraft speed is large and negative, or around four times the PDF width if the real updraft speed is large and positive.

We fixed this bug in the ARG (DIAG) activation scheme (from UM version 11.7) by redefining the minimum updraft in the PDF that is sampled as

$$w_{min} = \max(0, \bar{w} - 2\sigma_w) \tag{S2}$$

instead of zero, and the maximum as

$$w_{max} = \max(4\sigma_w, \bar{w} + 2\sigma_w) \tag{S3}$$

instead of $4\sigma_w$, to preserve existing behaviour as far as possible but still ensure that the PDF is still sampled in strong updrafts.
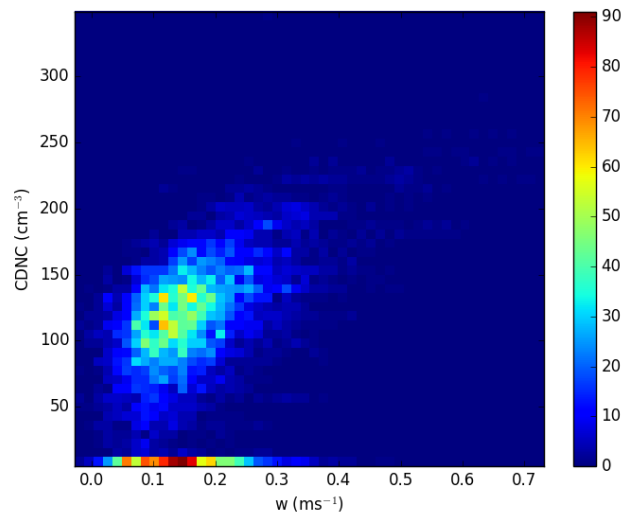
Figure S15. Correlation of updraft w with cloud droplet number (CDNC) calculated with the ARG (DIAG) activation scheme at low altitudes (below 900 m) for the 7 km-resolution simulation, as a two-dimensional histogram of model grid cells. At or close to cloud base, the updrafts can still be significant compared to the minimum updraft width, and consequently the PDF is not always fully sampled. All times are used (not just midday on 19 August) to increase the statistics available.